Rates of travertine formation at Fossil Creek, AZ: Baseline monitoring and implications for future research

Adam Schwarz
Department of Geology, Center for Environmental Science and Education
Northern Arizona University

Advisor: Rod Parnell

Abstract

This study's objective was to quantify rates of travertine formation at Fossil Creek, AZ. Travertine is a form of calcite ($CaCO_3$) that precipitates directly from supersaturated spring water as dissolved CO_2 is removed from the water by agitation or algal photosynthetic uptake (Malusa et al.,2003). Flow diversion for hydroelectric power generation has removed the water that replenishes the travertine system from the upper reach of Fossil Creek starting below Fossil Dam. During the summer of 2004 in two distinct CO_2 outgassing reaches, stainless steel, copper, and travertine tile substrates were anchored to travertine structures in the stream. The substrates were harvested after 74-120 days, dried, reweighed, and analyzed for percent inorganic and organic carbon using a Flash EA 1112 Elemental Analyzer. Water quality measurements were taken at each site and major cation and anion concentrations were determined in the lab. Analyses of calcite precipitation rates by substrate yielded ranges for the stainless steel, copper, and travertine tile substrates of $2.28\text{x}10^{-9}$-$1.52\text{x}10^{-8}$ g/cm^2/s, $1.10\text{x}10^{-9}$-$1.28\text{x}10^{-8}$ g/cm^2/s, and $4.76\text{x}10^{-9}$-$5.16\text{x}10^{-8}$ g/cm^2/s, respectively. Saturation index of calcite was found to increase with distance downstream, and was generally higher for the lower reach than the upper reach. Active travertine precipitation is expected to return to the upper reach, just below Fossil Dam once flow is restored. The data collected during this study will be used as a baseline for monitoring of ecosystem response to dam decommissioning and flow restoration scheduled for June, 2005.

Introduction

Fossil Creek, located in central Arizona, is a perennial travertine- depositing stream. "Travertine is a dense, finely crystalline massive or concretionary limestone, of white, tan or cream color, often having a fibrous or concentric structure and splintery fracture, formed by rapid chemical precipitation of calcium carbonate from solution in surface and ground waters, as by agitation of stream water or by evaporation around the mouth or in the conduit of a spring" (Bates and Jackson, 1987). Baseflow at Fossil Creek is provided by a group of spring vents collectively known as Fossil Springs. Fossil Springs emanate from the Pennsylvanian Naco Limestone and provide a near constant discharge of 1219 l/s to the stream (Malusa et al., 2003).

In the early 1900's, the Arizona Power Company capitalized on the steady baseflow of the springs and developed the stream for hydroelectric power generation. Construction on the project began in 1908, with the diversion of spring water by a flume to the Verde River at Childs (APS, 2004). The power plant at Childs was brought online in November of 1909, producing 2.8 megawatts of electrical power (Monroe, 2001). In 1914, construction began on a second plant at Irving to appease increased energy demand from mining in the Verde Valley. By the early 1920s, the plants supplied 70 percent of the power in Phoenix as well (Monroe, 2001). The plants have continued to supply 7 megawatts of power to Arizona to this day, but now only account for less than 0.1 percent of Arizona's energy generation (FERC, 2003).

All hydroelectric projects in the U.S. are required to be licensed by the Federal Energy Regulatory Commission (FERC). In 1992, APS filed an application for renewal of their license for the Childs-Irving Project. In 1997, FERC issued a Draft Environmental Assessment (DEA) on the relicensing proposal, considered the alternative of retiring the project, but recommended that a new license be issued (FERC, 2003). After issuance of the relicensing DEA, APS entered into discussions with the Forest Service and the objectors to the relicensing proceeding including American Rivers, the Center for Biological Diversity, and the Yavapai-Apache Nation. As a result, APS and the other parties filed an Offer of Settlement on September 15, 2000 signed by APS, American Rivers, the Center for Biological Diversity, the Yavapai-Apache Nation, the Arizona Chapter of the Nature Conservancy, the Northern Arizona Audubon Society, and the Arizona Riparian Council (FERC, 2003). APS filed an application to surrender the license and implement removal of the dam and restoration to the satisfaction of FERC and the Forest Service by December 31, 2009. Termination of power generation and restoration of full flows was scheduled for December 31, 2004, but delays have pushed this date back until June, 2005.

The decision to shut down the Childs-Irving hydroelectric facilities and restore full flows to Fossil Creek has important implications at the local, state and national level. Restoration actions following the decommissioning can serve as elements of a model for restoration of riparian ecosystems elsewhere that have been disturbed by flow diversion. In order to study the ecological consequences of restoring full flows to Fossil Creek, Northern Arizona University was awarded a grant by the Nina Mason Pulliam Charitable Trust entitled *A Comprehensive Monitoring Plan for Fossil Creek Watershed Restoration: a Model for Decommissioning Hydropower Facilities in the 21st Century* (Verde Watershed Research and Education Program, 2004). Part of this plan is to collect pre-decommissioning data regarding travertine formation rates to serve as a baseline for continued monitoring and research.

The water that emanates from Fossil Springs has an unusual geochemical signature that allows it to deposit travertine (Malusa et al., 2003). Travertine typically forms pool and dam structures which dramatically alter stream morphology by overprinting the typical Southwestern stream riffle and pool morphology. They provide more habitat for aquatic plants and animals, and increase primary and secondary productivity in the ecosystem by increasing leaf litter decomposition rates and algal productivity (Malusa et al. 2003; Marks et al., 2005). Other examples of travertine depositing streams in the USA include Mammoth Hot Springs in Yellowstone National Park, Montana, and Havasu Creek, Supai Reservation, Arizona (Malusa et al., 2003).

Travertine formation begins when percolating rain water interacts with the soil zone, carbonate aquifers, organic material, or regional geothermal activity to take up CO_2, which converts to CO_2 aqueous and H_2CO_3 (Malusa et al., 2003). H_2CO_3 increases dissolution of carbonate rocks, further elevating dissolved inorganic carbon concentrations in the water. The steep concentration gradient between atmospheric CO_2 and the higher dissolved CO_2 in water emerging from an aquifer initiates outgassing (Jacobson and Langmuir, 1970 and Langmuir, 1971). As the water's CO_2 concentration moves toward equilibrium through outgassing, the water becomes supersaturated with $CaCO_3$, eventually reaching a level high enough to begin precipitation. When this level is exceeded, a kinetic barrier is surpassed and $CaCO_3$ precipitates to form travertine deposits (Stumm and Morgan, 1996 and Dandurand et al., 1982). In 1996, Malusa et al. (2003) determined that in spite of flow diversion, potential for travertine formation at Fossil Creek still exists in the reaches immediately below the dam and below the Irving power plant.

Under conditions of flow diversion, travertine predominantly formed in the lower reach, below the Irving power plant, where partial flow of 43 l/s is returned to Fossil Creek. Limited travertine formation occurs in the upper reach, below Fossil Dam, from 5.6 l/s of seepage flow over the dam (Malusa et al., 2003). Restoration of full flow should return the focus of travertine formation to the upper reach of Fossil Creek, starting just below Fossil Dam.

This study was conducted to determine rates of travertine formation at eight locations along both these reaches within Fossil Creek. The effect of biological activity on travertine deposition rates at Fossil Creek is assessed in this study. Emeis et al. (1987) showed the importance of biological uptake of CO_2 in travertine deposition. Emeis et al. (1987) found that more precipitation occurred on stainless steel substrates than copper (an algaecide) substrates. Water quality data were also collected to assess the current (pre-decommissioning) flux of calcium carbonate in the system. These data will serve as a baseline for monitoring ecosystem response to dam decommissioning and removal at Fossil Creek scheduled for June, 2005.

Materials and Methods

A reach of Fossil Creek starting at the springs and continuing for approximately 15 km downstream was studied to determine rates of travertine formation (Fig.1). A control site (site 1) was chosen above the travertine precipitation zone just downstream from where the channel receives total baseflow. Two distinct CO_2 outgassing reaches are present within the overall reach. Three sites (sites 2,3,4) were chosen between Fossil Dam and the Irving power plant where travertine precipitation should increase following flow restoration. Three sites (sites 5,6,7) were chosen below the Irving power plant where flow and precipitation is currently higher but should decrease with flow restoration. A site was also chosen below the travertine precipitation zone (site 8).

Rates of travertine formation were determined from travertine precipitation on artificial substrates. Stainless steel and copper Chore Boy scrubbing pads and 11cm x 11cm x 0.5 cm travertine tiles were weighed and their surface areas estimated using a micrometer and simple geometry prior to emplacement in the stream. In May and June of 2004, four replicates of each substrate type were placed in Fossil Creek at the eight site locations. Substrates were placed in pools within travertine dam complexes. At sites where travertine dam structures were absent (sites 1, 3, 4, and 8), similar depth and flow pattern to those substrates placed within dams was used as criteria for choosing sampling locations.

Substrates were removed from Fossil Creek after 74 to 120 days. The substrates were dried at 70° C for 24 hours to complete dehydration, then reweighed. Gross travertine accumulation rates are reported as grams of accrual per cm^2 per second ($g/cm^2/s$).

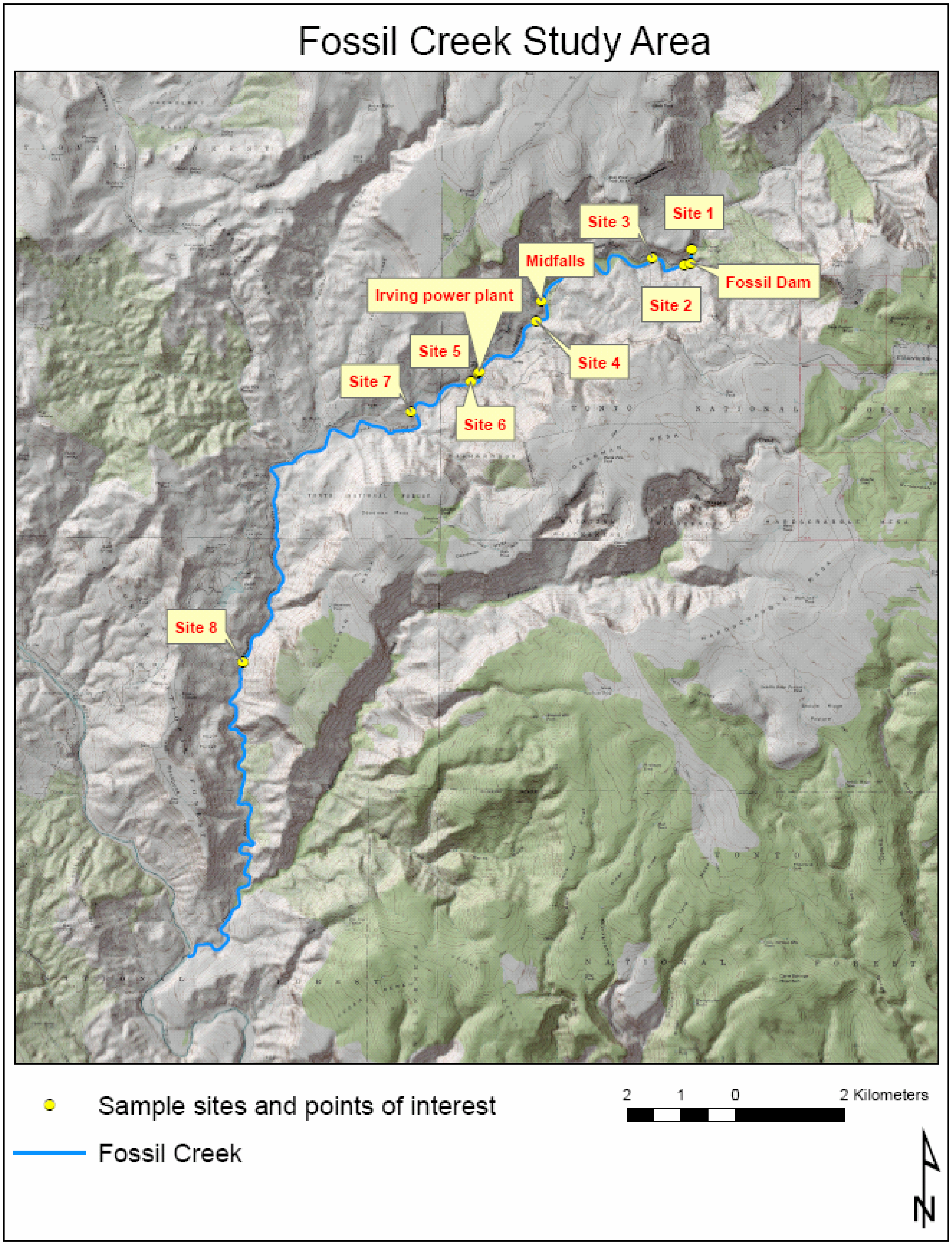

Figure 1. Fossil Creek study area. The upper outgassing reach runs from Fossil Dam to the Irving power plant. The lower reach starts below the power plant and ends at site 8.

Solid deposition on substrates was collected and ground to a fine powder for organic and inorganic carbon analysis of the total accrual. Total carbon was measured using a Flash EA 1112 Elemental Analyzer. Samples were digested in 1 N hydrochloric acid to remove inorganic carbon, reweighed and normalized for entrained Cl^-, then analyzed in the Flash EA 1112 Elemental Analyzer to obtain total organic carbon. Solid inorganic carbon was obtained by subtracting total organic carbon from total carbon:

$$TIC= TC-TOC$$

The total inorganic carbon concentration was used to determine percent $CaCO_3$. This value is defined as the travertine precipitation rate and is reported as grams of $CaCO_3$ per cm^2 per second ($g/cm^2/s$). The total accrual weight is the sum of travertine precipitation plus organic matter plus detrital inorganic matter accumulation.

Three water samples were taken at each site (excluding site 8) on August 5, 2004, and from site 3 on August 9, 2004. Two samples were filtered with a 0.45 micron filter into acid washed plastic water bottles for cation and anion analysis. One of these was spiked with pure nitric acid to bring pH below 2, preventing negative functional group sorption of the cations. One sample was filtered with a 0.45 micron glass filter into a glass bottle for total dissolved carbon analysis. Temperature, pH, and conductivity measurements were taken on site.

Total dissolved organic and inorganic carbon were analyzed using a Dohrmann Phoenix 8000 carbon analyzer. Equilibrium speciation calculations were performed to determine concentrations of H_2CO_3, HCO_3^-, and CO_3^{2-}. Cations were analyzed using a Perkin-Elmer 560 Atomic Absorption Spectrophotometer to determine concentrations of Ca^{2+}, Mg^{2+}, Na^+ and K^+. Anions were analyzed using a Dionex DX-100 Ion Chromatograph to determine concentration of Cl^- and SO_4^{2-}. Ion concentrations were converted from mg/L to meq/L to obtain charge balance. The charge balance is defined as ($\sum$anions meq/L -$\sum$cations meq/L)/($\sum$anions + $\sum$cations).

Saturation index (SI), defined as the ion activity product divided by the solubility product at a given temperature, was calculated for calcite at each site. A $\log_{10}$(SI) of 0 represents equilibrium, values below zero indicate an undersaturated solution, and values greater than zero indicate supersaturation. P_{CO_2} was calculated assuming equilibrium for water samples. Both of these values are reported as $\log_{10}(P_{CO_2})$ and $\log_{10}(SI)$.

Results and Discussion

$CaCO_3$ precipitation

Calcite precipitation was undetectable on artificial substrates at site 1 due to the close proximity of the site to the springs, preventing sufficient CO_2 outgassing for precipitation (Table 1). Stainless steel and travertine substrates experienced small amounts of detrital mass accumulation, and copper substrates actually experienced a deduction in mass due to degradation of the substrate.

Calcite precipitation on all substrates had initiated by site 2, which yielded the highest rates for the upper outgassing reach. These rates decreased at site 3, then increased again at site 4 (Table 1). The increase at site 4 may be due to an increased outgassing effect from the midfalls (Fig. 2) approximately 0.5 km upstream from the site, or addition of highly supersaturated spring waters between sites 3 and 4.

Table 1. Travertine accumulation and calcite precipitation rates. Inorganic carbon is reported as grams of calcite per cm^2 per second. Rates are replicate means for each site. SS and Cu stand for stainless steel substrates and copper substrates, respectively.

ID (distance downstream (km))	SS total accrual ($g/cm^2/s$)	SS inorganic carbon ($g/cm^2/s$)	Cu total accrual ($g/cm^2/s$)	Cu inorganic carbon ($g/cm^2/d$)	Travertine tile total accrual ($g/cm^2/s$)	Travertine tile inorganic carbon ($g/cm^2/s$)
Site 1 (0.0)	3.69E-10	0.00E+00	-9.89E-11	0.00E+00	2.71E-10	0.00E+00
Site 2 (0.366)	1.65E-08	1.52E-08	1.77E-08	1.22E-08	1.67E-08	1.74E-08
Site 3 (1.11)	7.01E-09	5.11E-09	4.30E-09	3.61E-09	1.55E-08	1.46E-08
Site 4 (4.52)	7.95E-09	6.96E-09	7.13E-09	6.12E-09	1.70E-08	1.51E-08
Site 5 (0.04)	5.75E-09	5.09E-09	1.81E-09	1.10E-09	1.48E-08	1.13E-08
Site 6 (0.35)	7.70E-09	6.78E-09	5.71E-09	4.96E-09	5.64E-08	5.16E-08
Site 7 (1.71)	1.16E-08	9.96E-09	1.53E-08	1.28E-08	1.85E-08	1.60E-08
Site 8 (9.5)	5.45E-09	2.28E-09	7.41E-09	4.76E-09	8.79E-09	4.76E-09

In the lower outgassing reach, calcite precipitation occurred on all substrates at site 5, increased at site 6, increased more at site 7 on stainless steel and copper substrates but decreased between sites 6 and 7 on travertine tile substrates. Rates on all substrates decreased between sites 7 and 8 (Table 1; Fig. 2).

Travertine precipitation was generally highest on the travertine tile substrates. This may be due to their planar surface geometry not sealing off any available nucleation surface, and due to calcite being preferred as a nucleation site for further calcite precipitation.

There is a strong correlation between mass of calcite and the total accrual mass formation rates on all substrate types (Figs. 4, 5, 6). R^2 values for stainless steel, copper and travertine tile substrates are 0.965, 0.968, and 0.989, respectively, significant at a 95% confidence level. This correlation shows that an increase in the total accrual rate accompanies an increase in calcite precipitation or vice versa.

Difference in precipitation rates on stainless steel and copper substrates

The importance of algal photosynthetic uptake of CO_2 on travertine formation was assessed by comparing rates of calcite precipitation on stainless steel and copper substrates. Copper should act as an algaecide, preventing algal colonization and uptake of CO_2 through photosynthesis. It was hypothesized that calcite precipitation rates would be reduced on copper substrates.

The difference in calcite precipitation rates on stainless steel and copper substrates was found to be insignificant at all sites except site 5 (Fig. 3). The results suggest that stainless steel substrates at sites 2, 3, 4, and 6 may have been preferred for calcite precipitation but the differences are not significant. These results show that the copper substrate did not act as an effective algaecide, that algal material migrates to the surface of the travertine as it accumulates and is not incorporated into the overall travertine structure, or that algal photosynthetic uptake of CO_2 at Fossil Creek is more influential on the bulk P_{CO2} concentration of the water than affecting precipitation on the substrate on which the algae resides.

Saturation index, P_{CO2} and ion loss

$Log_{10}(SI)$ of $CaCO_3$ in water at site 1 was near equilibrium with a value of 0.02. In the upper outgassing reach, SI increased with distance downstream from 0.39 at .0.37 km to 0.65 at 4.52 km. In the lower reach, SI increased from 0.62 at 0.04 km to 0.95 at 1.71 km (Table 2).

P_{CO2} was highest at site 1 (Table 2). P_{CO2} decreases downstream in both reaches with distance downstream. The calculated values are within the range observed by Malusa et al. (2003). The decrease in P_{CO2} is due to outgassing of CO_2 from turbulent flow and algal photosynthetic uptake of CO_2, both of which remove dissolved CO_2 from solution.

Table 2. Aqueous chemical data from Fossil Creek sampling sites. All water samples were taken on August 5, 2004, except site 3 taken August 9, 2004.

ID (distance downstream (km))	temp (°C)	pH	conductivity (µS/cm)	DIC (mg/L)	H_2CO_3 (mg/L)	HCO_3^- (mg/L)	CO_3^{2-} (mg/L)	Ca^{2+} (mg/L)	Log(SI) $CaCO_3$	Log (P_{CO_2})	ALK (M/L)
Site 1 (0.00)	21.4	6.87	749	496.2	122.7	373.3	0.11	79.23	0.02	-1.52	0.0061
Site 2 (0.336)	21	7.35	675	379.0	37.2	341.5	0.31	66.42	0.39	-2.04	0.0056
Site 3 (1.11)	20.9	7.64	629	362.4	19.1	342.7	0.61	56.52	0.61	-2.33	0.0056
Site 4 (4.52)	22.3	7.94	543	299.3	8.1	290.1	1.04	36.96	0.65	-2.70	0.0048
Site 5 (0.04)	21.6	7.44	736	441.4	35.9	405.1	0.46	78.50	0.62	-2.05	0.0067
Site 6 (0.35)	21.6	7.65	714	398.0	20.6	376.8	0.69	74.39	0.78	-2.29	0.0062
Site 7 (1.71)	21.6	8	624	335.8	8.0	326.5	1.34	56.28	0.95	-2.71	0.0054

Calcium and bicarbonate concentrations decreased as pH increased with distance downstream for both outgassing reaches. As dissolved CO_2 is removed from solution, SI increases until the water cannot hold dissolved $CaCO_3$ in solution, and precipitation of calcite is initiated, effectively reducing concentration of Ca^{2+} and HCO_3^- in the water. The slope of ion loss was found to be steeper in the lower reach, suggesting that increased rates of $CaCO_3$ precipitation are occurring in the lower reach (Fig. 7).

Concentrations of magnesium, potassium, sodium and chloride increased at site 4, suggesting spring input between sites 3 and 4 or evaporative concentration of spring waters, but stayed approximately constant over the rest of the sampling area (Table 3). Sulfate concentrations decreased in both reaches with distance downstream, suggesting that some form of $Ca(SO_4)$, possibly gypsum, may be precipitating along with $CaCO_3$, or being removed by biologic activity.

Table 3. Major ion concentrations and charge balance. All sites fall within accepted 15% range of precision.

ID (distance downstream (km))	Ca^{2+} mg/L	Mg^{2+} mg/L	K^+ mg/L	Na^+ mg/L	HCO_3^- mg/L	CO_3^{2-} mg/L	Cl^- mg/L	SO_4^{2-} mg/L	charge balance %
Site 1 (0.00)	79.2	40.2	1.1	8.2	373.3	0.11	8.5	25.1	11.0
Site 2 (0.336)	66.4	40.1	1.3	6.6	341.5	0.31	8.9	24.3	9.0
Site 3 (1.11)	56.5	41.5	1.3	8.9	342.7	0.61	9.3	21.9	4.7
Site 4 (4.52)	37.0	42.0	2.2	11.1	290.1	1.04	10.4	10.8	10.0
Site 5 (0.04)	78.5	40.3	1.1	6.4	405.1	0.46	8.5	25.9	1.3
Site 6 (0.35)	74.4	40.3	1.3	6.7	376.8	0.69	8.3	25.3	5.6
Site 7 (1.71)	56.3	40.1	1.1	6.4	326.5	1.34	8.5	24.8	4.2

Summary

Travertine formation rates at eight locations along Fossil Creek were quantified. Calcite precipitation occurred on at all sampling sites on all artificial substrates except site 1. Absence of calcite precipitation at site 1 is due to the site's close proximity to the springs. Insufficient outgassing occurred to induce calcite precipitation. Calcite precipitation rates increase in both reaches after initial outgassing, then decrease as calcium and bicarbonate concentrations are reduced downstream (Table 1; Fig. 2). Strong correlation of total accrual and calcite precipitation rates were found for all substrate types (Figs. 4,5,6). Highest rates of travertine formation occurred in the lower reach and on travertine tile substrates (Fig. 2).

The importance of algal photosynthetic uptake of CO_2 on travertine formation was investigated. Differences in calcite precipitation on stainless steel and copper substrates were found to be insignificant except at site 5 (Fig. 3). These results show that the copper substrate did not act as an effective algaecide, that algal material migrates to the surface of the travertine as it accumulates and is not incorporated into the overall travertine structure, or that algal photosynthetic uptake of CO_2 at Fossil Creek is more influential on the bulk P_{CO_2} concentration of the water than affecting precipitation on the substrate on which the algae resides.

Water quality measurements were taken and concentrations of major dissolved ions were determined (Table 2). Ca^{2+} and HCO_3^- concentrations were found to decrease downstream in both reaches as these ions are precipitated from solution as $CaCO_3$. The rate of ion loss was faster in the lower reach due to higher discharge being more turbulent, allowing faster outgassing of CO_2. Mg^{2+}, Na^+, K^+, and Cl^- stayed relatively constant, but SO_4^{2-} concentrations decreased downstream, suggesting that $Ca(SO_4)$ may be precipitating along with $CaCO_3$.

Saturation index of calcite increased with distance downstream with higher values in the lower reach (Table 2). P_{CO_2} decreased downstream and turbulent flow and biotic uptake remove CO_2 from solution (Table 2).

Conclusion

Current rates of travertine precipitation at Fossil Creek are higher in the lower reach just downstream of the Irving power plant than in the upper reach just below Fossil

Dam. The higher rate of precipitation reflects higher discharge in the lower reach being more turbulent, allowing more rapid outgassing of dissolved CO_2, which increases pH and SI and allows $CaCO_3$ precipitation. Once full flows are restored, $CaCO_3$ precipitation rates should increase in the upper reach due to higher discharge carrying more dissolved $CaCO_3$ per unit time, more turbulent flow facilitating faster CO_2 outgassing, and more wetted surface area for algal colonization and photosynthetic uptake of CO_2.

The importance of algal colonization directly on travertine structures in removing CO_2 from solution and facilitating $CaCO_3$ precipitation was found to be insignificant by this study; however, the impact of algal photosynthetic uptake of CO_2 on changing the overall chemistry of the water should not be disregarded. These results present an opportunity for redesign of this aspect of the experiment and more study on the effects of biological activity on travertine formation.

Changes in stream morphology associated with newly formed travertine structures should be relatively instantaneous once full flows are restored. Once calcite nucleation has initiated at preferred precipitation sites, rapid aggradation should persist as long as calcium and bicarbonate ions are available for precipitation. Continuous monitoring of precipitation rates and channel topography will give great insight into changes in stream morphology and ecosystem response associated with dam decommissioning and flow restoration.

Future research and monitoring should continue to explore biological influence on travertine formation with alternatives methods for algal exclusion from substrates. Also, as travertine formation rates increase and the spatial distribution of dams increases, it will be beneficial to include more sampling sites for a more comprehensive view of travertine precipitation dynamics along the portion of the stream where active precipitation will be occurring. Future work will be essential in gaining a detailed understanding of travertine formation dynamics and its role in the aquatic ecosystem at Fossil Creek.

References

Arizona Public Service (APS). 2004. A stream is reborn: Decommissioning the Childs-Irving power plant. Retrieved in March 2005 from http://www.aps.com/my_community/StoryArchive/StoryArchive_18.html.

Bates, R.L. and Jackson, J.A. 1987. Glossary of Geology. American Geological Institute, Alexandria, VA.

Dandurand, J.L., Gout, R., Hoefs, J., Menschel, G., Schott, J. and Usdowski, E. 1982. Kinetically controlled variation of major components and carbon and oxygen isotopes in a calcite-precipitating spring. *Chem. Geol.* **36**: 299–315.

Emeis, K.C., Richnow, H.H. and Kempe, S., 1987. Travertine formation in Plitvice National Park, Yugoslavia: chemical versus biological control. *Sedimentology.* **34**, pp. 595–609.

Federal Energy Regulatory Commission. 2003. Draft Environmental Assessment for Surrender of License, Childs-Irving Project. FERC Division of Hydropower-Environment and Engineering, Washington, DC.

Jacobson, R.L. and Langmuir, D., 1970. The chemical history of some spring waters in carbonate rocks. *Ground Water* **8**: 5-9.

Langmuir, D., 1971. The geochemistry of some carbonate groundwater in central Pennsylvania. *Geochim. Cosmochim. Acta* **35**: 1023–1045

Malusa, J., Overby, S.A., Parnell, R.A. 2003. Potential for travertine formation: Fossil Creek, AZ. *Applied Geochemistry* **18**:1081-1093.

Marks, J.C., Parnell, R., Carter, C., Dinger, E.C., Haden, A. 2005. Interactions between geomorphology and ecosystem processes in travertine stream- implications for dam decommissioning in Fossil Creek, Arizona. Manuscript in submission.

Monroe, S.A. 2001. A Wonderful Water Power. Pine-Strawberry Archeological & Historical Society. Pine, AZ.

Stumm, W. and Morgan, J.J. 1996. Aquatic chemistry. John Wiley & Sons, New York.

Figures

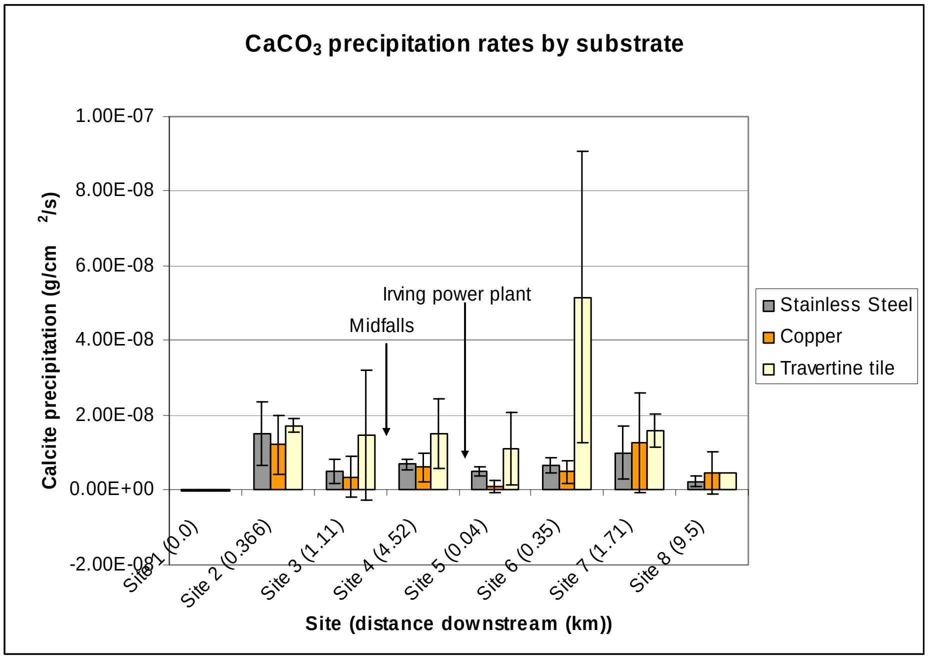

Figure 2. Calcite precipitation rates at sampling sites by substrate. Bars are 1 standard deviation of the replicate mean. The lower outgassing reach starts below the Irving power plant.

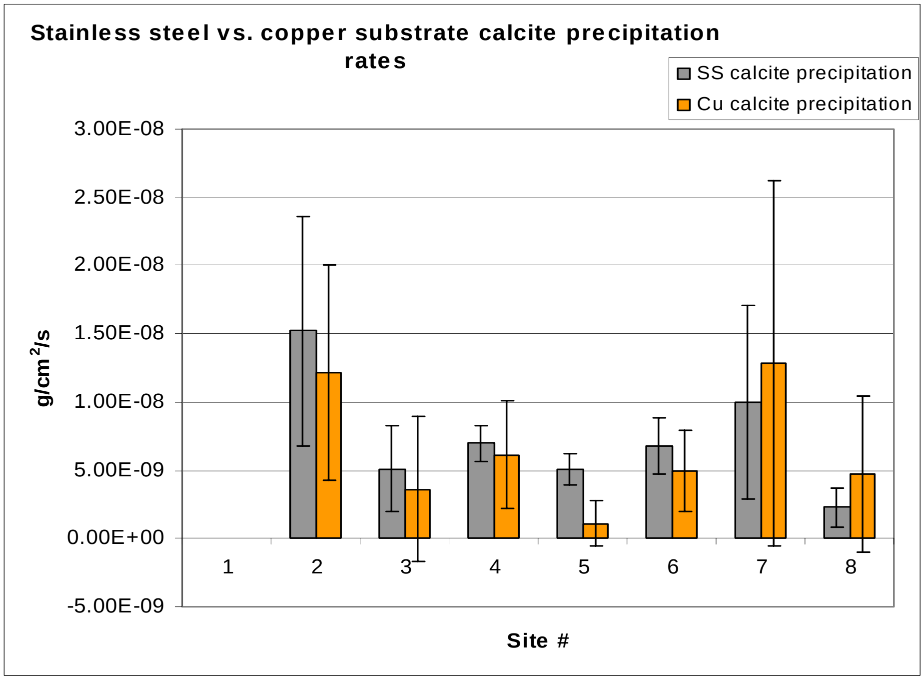

Figure 3. Difference in calcite precipitation rates on stainless steel and copper substrates. Bars are 1 standard deviation of the replicate mean.

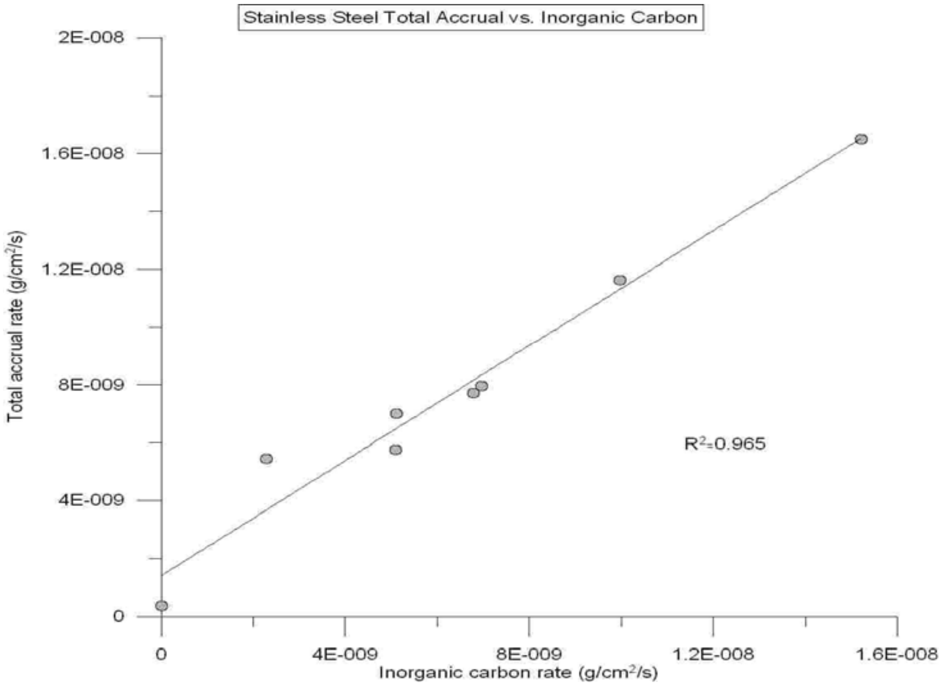

Figure 4. Total mass accumulation rates vs. calcite precipitation rates on stainless steel substrates. Correlation is significant with and R^2 value of 0.965.

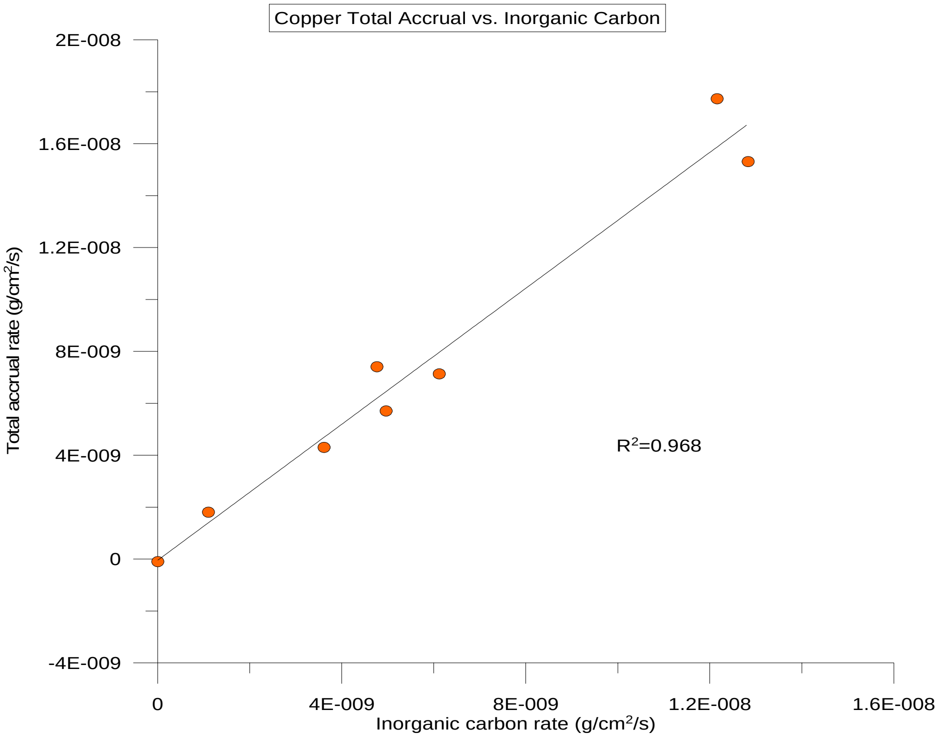

Figure 5. Total mass accumulation rates vs. calcite precipitation rates on copper substrates. Correlation is significant with and R^2 value of 0.968.

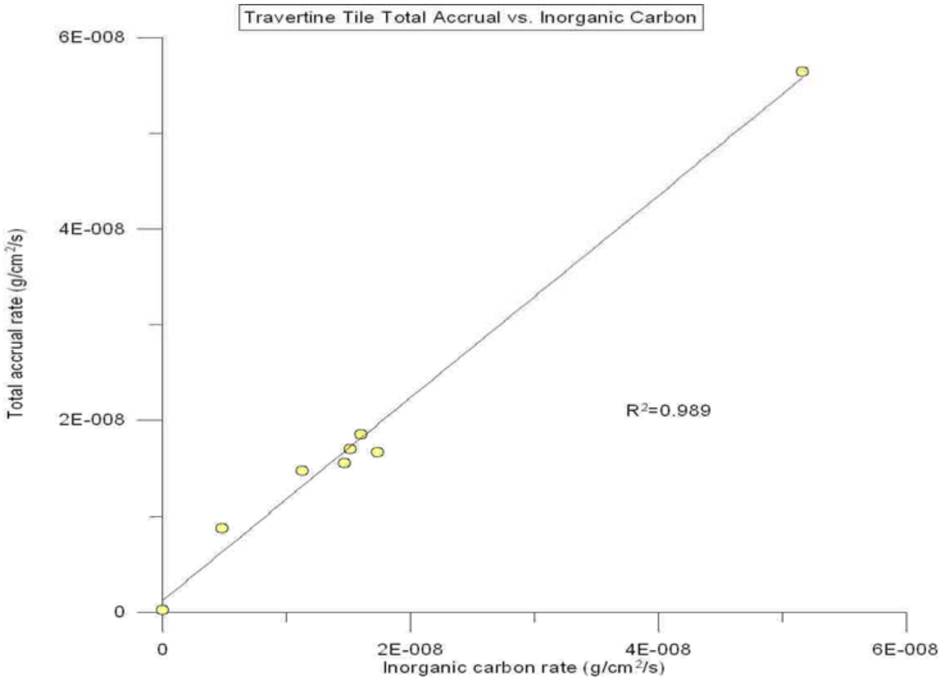

Figure 6. Total mass accumulation rates vs. calcite precipitation rates on travertine tile substrates. Correlation is significant with and R^2 value of 0.989.

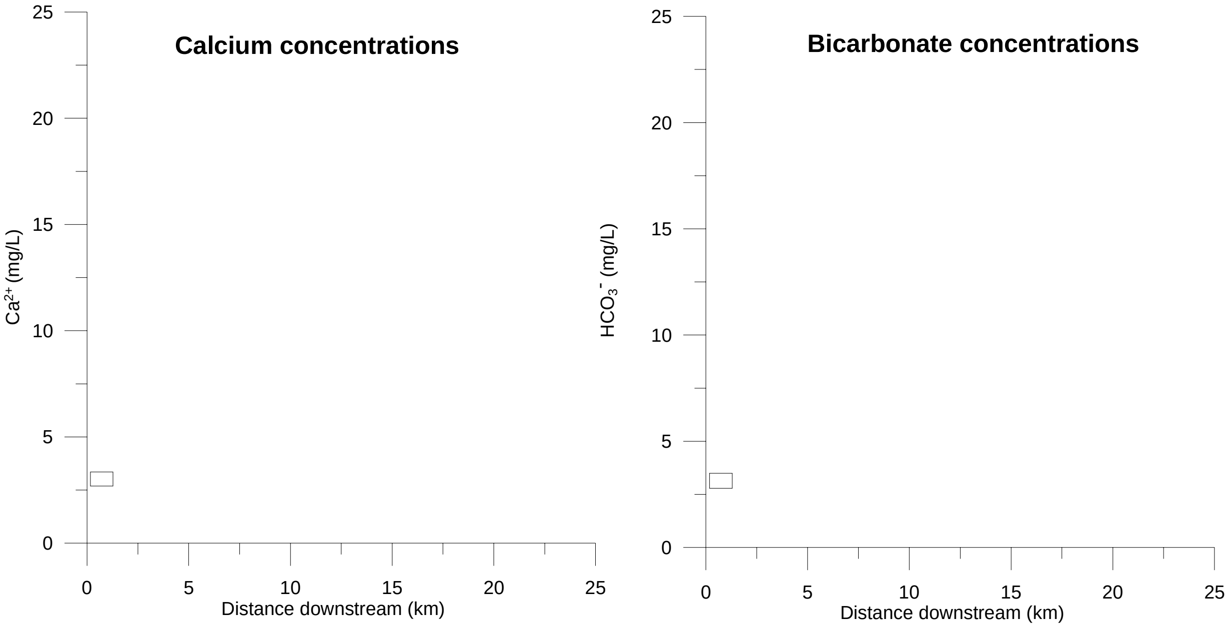

Figure 7. Dissolved calcium and bicarbonate concentrations in water sampled on August, 5th, 2004 (sites 1,2,4,5,6,7) and August 9th, 2004 (site3).